Macroscopic Modeling of Mn-Zn Ferrites Based on Analytical Dynamic Material Models

Reda Elkhadrawy[1], Joonas Vesa[1], Vasiliki Tsakaloudi[2], and Paavo Rasilo[1]
[1]Electrical Engineering Unit, Tampere University, FI-33720 Tampere, Finland
[2]Laboratory of Inorganic Materials, Centre of Research and Technology Hellas, Thessaloniki, Greece

We propose a semi-analytical approach for modeling the macroscopic electromagnetic behavior of Mn-Zn ferrite cores under both dielectric and magnetic excitations. First, analytical material models are provided for calculating the effective parameters, i.e., complex resistivity and complex reluctivity by solving the electromagnetic fields in a single simplified grain and its boundary layer. The effective parameters are then used in 2-D axisymmetric finite element (FE) models for solving the full-wave electromagnetic field equation in a cross-section of a ferrite core under both dielectric and magnetic excitations. The simulated dielectric and magnetic impedances of a ferrite core are validated against measurements.

***Index Terms*—complex permeability, complex permittivity, core losses, ferrites, finite element method**

I. Introduction

MN-ZN ferrites offer low losses at low cost for high-frequency inductors, transformers, and common mode chockes used in power electronics [1]. Ferrites are sintered materials, and they have a heterogeneous polycrystalline microstructure with conductive grains and very resistive grain boundaries. The microstructure has a significant impact on the macroscopic electromagnetic behavior of the material [1]. Thus, modeling ferrite cores while considering the heterogeneous structure is essential.

Modeling such complex structures using classical numerical methods such as the finite element (FE) method (FEM) is computationally very expensive. Alternative approaches in the literature are based on either equivalent circuit models [2] or multiscale methods [3]-[7]. Dimier and Biela made use of an RC equivalent circuit to model the macroscopic complex permittivity for calculating the eddy-current losses in a ferrite core [2]. Bottauscio et al. discussed several approaches based on homogenization and multiscale methods for electromagnetic modeling of heterogeneous soft magnetic materials [5]. Niyonzima et al. presented a heterogeneous multiscale method for modeling the behavior of electromagnetic fields in soft magnetic composites (SMC) [6]. Ren et al. proposed a homogenization strategy to define the equivalent electromagnetic properties of SMC for calculating the eddy current losses or designing electromagnetic devices using structural analysis tools [7]. The equivalent circuit models are insufficient for studying how the microstructure of the core affects the macroscopic behavior. On the other hand, the multiscale models are still time-consuming since the fields have to be solved first in the so-called mesoscale and then upscaled to the macroscale.

From the practical point of view, there is still a need for even faster approaches for considering the heterogeneous grain structure. The main contribution of this work is to develop analytical material models for the effective electromagnetic parameters, i.e., complex resistivity and complex reluctivity of Mn-Zn ferrites. Such material models can be used in FE models for simulating the macroscopic behavior of ferrite cores. The proposed material models follow the idea of the reluctivity model presented in [8]. The main difference here is that the material models are developed in a more general manner since, in ferrites, both the conductivity and permittivity of the grains and the boundaries have a significant effect on the material behavior. First, we derive the material models by solving the electromagnetic fields in a single grain/boundary cell analytically. The microstructure of the core is considered in the material models through the geometrical and electromagnetic parameters of the grains and the boundaries. The proposed material models are then used for estimating the effective parameters which are utilized in 2-D axisymmetric FE models for simulating the macroscopic electromagnetic behavior of a ferrite core under both dielectric and magnetic excitations. For validation, the simulated dielectric and magnetic impedances of a toroidal ferrite core are compared against measurements.

Corresponding author: Reda Elkhadrawy (e-mail: reda.elkhadrawy@tuni.fi).

II. Computational Models

A. Macroscopic Models

Cylindrical coordinates (r, φ, z) and frequency domain analysis are adopted. 2-D axisymmetric FE models are constructed for solving the electromagnetic full-wave

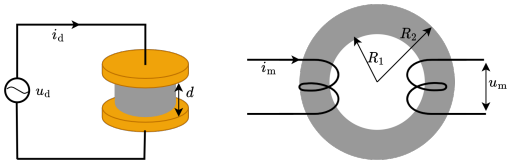

(a) Dielectric excitation. (b) Magnetic excitation.

Fig. 1: Schematics of the measurement setups with different excitations.

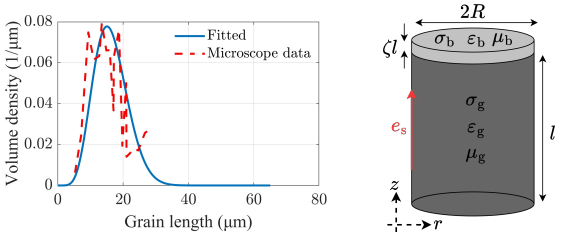

(a) (b)

Fig. 2: Grain size distribution obtained from microscope images and fitted beta distribution (a) and a schematic of a single grain/boundary cell (b).

equation in the rectangular cross section of a ferrite core. From Maxwell's equations, the governing equation for the magnetic field strength $\boldsymbol{H}$ reads

$$\nabla \times (\rho_{\text{eff}} \nabla \times \boldsymbol{H}) + j\omega \nu_{\text{eff}}^{-1} \boldsymbol{H} = 0, \tag{1}$$

where ρ_{eff} and ν_{eff} are the effective complex resistivity and reluctivity, respectively, j is the imaginary unit, and $\omega = 2\pi f$ is the angular frequency. The effective material parameters take into account the grain-scale behavior of the material. We discuss them later.

The exact representation of the boundary conditions for solving (1) depends on if the sample is excited by dielectric or magnetic excitation and whether the sample is a disk or a toroid. When the core is under a dielectric (subscript d) excitation, as shown in Fig. 1a, the boundary conditions read

$$H_\varphi(R_1, z) = 0, \;\; H_\varphi(R_2, z) = \frac{i_\text{d}}{2\pi R_2}, \tag{2}$$

where i_d is the total current passing through the core and R_1 and R_2 are the inner and outer radii of the core, respectively. On the other hand, when the core is under a magnetic (subscript m) excitation as shown in Fig. 1b, the boundary conditions read

$$\begin{aligned} H_\varphi(R_1, z) = \frac{N_1 i_\text{m}}{2\pi R_1}, \; H_\varphi(R_2, z) = \frac{N_1 i_\text{m}}{2\pi R_2}, \\ H_\varphi(r, 0) = H_\varphi(r, d) = \frac{N_1 i_\text{m}}{2\pi r}, \end{aligned} \tag{3}$$

where i_m is the current in the winding, N_1 is the number of turns in the primary coil. Conditions (3) are only possible for a wound toroid. To summarize, (1) and (2) comprise the dielectric model and (1) and (3) comprise the magnetic model. The Galerkin FEM is used for discretizing both models with nodal elements for H_φ.

The dielectric and magnetic impedances of the ferrite samples $Z_{\text{d/m}}(\omega) = R_{\text{d/m}} + jX_{\text{d/m}}$ are calculated as

$$Z_{\text{d/m}}(\omega) = \frac{1}{|i_{\text{d/m}}|^2} \int_\Omega \left[\rho_{\text{eff}} \|\nabla \times \boldsymbol{H}\|^2 + j\omega \nu_{\text{eff}}^{-1} \|\boldsymbol{H}\|^2 \right] \text{d}\Omega, \tag{4}$$

where Ω is the core volume.

B. Material Models

The idea here is to define an equivalent homogenized material that has effective homogeneous parameters, i.e., $\rho_{\text{eff}}(\omega)$ and $\nu_{\text{eff}}(\omega)$. Such effective material parameters consider the heterogeneous structure of the material through their frequency-dependency. Earlier, an analytical material model for the effective reluctivity ν_{eff} in soft magnetic composites was developed [8], [9]. Some of those ideas are further developed here for a resistivity model ρ_{eff}. The grains are assumed to be cylinders of radius R and length $l = 2R$ as depicted in Fig. 2b. The electric field is treated as rotationally symmetric around the symmetry axis of the cylinder and translationally symmetric in the $z-$direction. Furthermore, the resistivity model considers axially symmetric current densities in the direction of the electric field. The equation of the electric field $\boldsymbol{e} = e(r)\hat{z}$ on a cross-section of a grain (subscript g), without the boundary layer (subscript b), reads [10]:

$$r^2 e'' + re' + \gamma^2 r^2 e = 0 \text{ and } e(R) = e_\text{s}, \tag{5}$$

where $\gamma^2 = -j\omega\mu_\text{g}\tilde{\sigma_\text{g}}$ and $\tilde{\sigma_\text{g}} = \sigma_\text{g} + j\omega\varepsilon_\text{g}$. Furthermore, μ_g, σ_g, and ε_g are the permeability, conductivity, and permittivity of the grain, respectively, and e_s is the excitation field. From the field solution, the current that passes from the grain to the boundary layer through the top surface is obtained by

$$I = 2\pi \int_0^R \tilde{\sigma_\text{g}} e(r) r \text{d}r = \frac{2\pi R \tilde{\sigma_\text{g}}}{\gamma} \frac{J_1(\gamma R)}{J_0(\gamma R)} e_\text{s}, \tag{6}$$

where J_0 and J_1 are the zero- and first-order Bessel functions of the first kind, respectively. Since ferrite material includes open porosity, a coefficient η where $0 < \eta \leq 1$ is introduced to model the volume fraction of the material. Hence, the effective cross-sectional area through which the current passes is $\pi R^2/\eta$, and the effective current density is given by

$$j_\text{eff} = \frac{I}{\pi R^2/\eta} = \frac{2\tilde{\sigma_\text{g}}\eta}{\gamma R} \frac{J_1(\gamma R)}{J_0(\gamma R)} e_\text{s}. \tag{7}$$

A single grain can be connected to another through the boundary layer using the concept of impedance network. The impedance of the boundary layer can be modeled by

$$Z_{\mathrm{b}} = \frac{\zeta l}{\tilde{\sigma}_{\mathrm{b}} \pi R^2}, \tag{8}$$

where $\tilde{\sigma_{\mathrm{b}}} = \sigma_{\mathrm{b}} + j\omega\varepsilon_{\mathrm{b}}$. Furthermore, ζ, σ_{b}, and ε_{b} are the relative thickness, conductivity, and permittivity of the boundary layer, respectively. Considering the current continuity through the grain and the boundary layer, the electric field in the boundary layer is

$$e_{\mathrm{b}} = \frac{Z_{\mathrm{b}} I}{\zeta l} = \frac{1}{\tilde{\sigma}_{\mathrm{b}} \eta} j_{\mathrm{eff}}. \tag{9}$$

The effective electric field strength e_{eff} over the grain/boundary cell of length $(1+\zeta)l$ is

$$e_{\mathrm{eff}} = \frac{\zeta l e_{\mathrm{b}} + l e_{\mathrm{s}}}{(1+\zeta) l}. \tag{10}$$

Substituting (7) and (9) into (10) gives

$$e_{\mathrm{eff}} = \underbrace{\frac{1}{(1+\zeta)\eta} \left(\frac{\zeta}{\tilde{\sigma}_{\mathrm{b}}} + \frac{\gamma R}{2\tilde{\sigma}_{\mathrm{g}}} \frac{J_0(\gamma R)}{J_1(\gamma R)} \right)}_{\rho_{\mathrm{eff,c}} \text{ of a single grain/boundary cell}} j_{\mathrm{eff}}. \tag{11}$$

So far we have focused on the resistivity of a single grain/boundary cell $\rho_{\mathrm{eff},c}$. It is not straightforward to generalize (11) into a resistivity of the whole material, consisting of grains of various sizes, described by a grain size distribution. Let us consider a sequence of grains sharing the same effective current density j_{eff}. An effective electric field over the whole sequence is defined as the electromotive force over the sequence divided by the length of the sequence. Hence, we may set

$$\rho_{\mathrm{eff}} = \frac{\int \rho_{\mathrm{eff,c}} l g(l) \mathrm{d}l}{\int l g(l) \mathrm{d}l}, \tag{12}$$

where g is a grain count density function.

Formulas (11)-(12) define our resistivity model. However, such a model is rather cumbersome to deal with. It was proposed in [9] to use for a reluctivity model an effective grain radius R_{eff} of the form

$$R_{\mathrm{eff}} = \frac{1}{2} \frac{(l_{\max} - l_{\mathrm{avg}}) l_{\mathrm{avg}}^2 - (2l_{\max} + l_{\mathrm{avg}}) l_{\mathrm{dev}}^2}{(l_{\max} - l_{\mathrm{avg}}) l_{\mathrm{avg}} - 3 l_{\mathrm{dev}}^2}, \tag{13}$$

where $l_{\max} = 100$ µm is the maximal grain length, and $l_{\mathrm{avg}} = 16.3$ µm and $l_{\mathrm{dev}} = 5$ µm are the expectation and the deviation of the grain lengths in a grain volume distribution. The grain size distribution shown in Fig. 2a reveals how much material volume is filled by grains of specific lengths. The effective radius lumps a beta-distributed collection of grains into one effective radius representing the whole material, and its value is $R_{\mathrm{eff}} = 6.4$ µm. Hence, the effective complex resistivity of the whole material reads

TABLE I: Geometrical and electromagnetic parameters

Parameter	Symbol	Value
Relative boundary thickness	ζ	2.8×10^{-4}
Grain relative permeability	μ_{g}	2887
Boundary relative permeability	μ_{b}	3
Grain conductivity	σ_{g}	64 S/m
Boundary conductivity	σ_{b}	3.6×10^{-5} S/m
Grain relative permittivity	ε_{g}	1.9
Boundary relative permittivity	ε_{b}	55.9

$$\rho_{\mathrm{eff}}(\omega) = \frac{1}{(1+\zeta)\eta} \left(\frac{\zeta}{\tilde{\sigma}_{\mathrm{b}}} + \frac{\gamma(\omega) R_{\mathrm{eff}}}{2\tilde{\sigma}_{\mathrm{g}}} \frac{J_0(\gamma(\omega) R_{\mathrm{eff}})}{J_1(\gamma(\omega) R_{\mathrm{eff}})} \right), \tag{14}$$

Following a similar approach as presented in [9], the effective complex reluctivity model reads

$$\nu_{\mathrm{eff}}(\omega) = \frac{1}{(1+\zeta)\eta} \left(\frac{\zeta}{\mu_{\mathrm{b}}} + \frac{\gamma(\omega) R_{\mathrm{eff}}}{2\mu_{\mathrm{g}}} \frac{J_0\left(\gamma(\omega) R_{\mathrm{eff}}\right)}{J_1\left(\gamma(\omega) R_{\mathrm{eff}}\right)} \right), \tag{15}$$

where μ_{b} is the permeability of the boundary layer.

III. Results and Discussion

Two disk-shaped (D) and two toroidal (T) Mn-Zn ferrite cores from the same batch are investigated in both dielectric and magnetic excitations. The cores are with outer diameter / inner diameter / height $(2R_2/2R_1/d)$ of 22/0/7.5, 11/0/7, 25/15/11, and 25/15/11 mm/mm/mm, and they are denoted as D1, D2, T1, and T2 respectively. Making use of microscope images, the grain size distribution is obtained and accordingly $l_{\max}$, l_{avg} and l_{dev} are estimated. The ferrite supplier reported that the porosity in the samples is about 5%, therefore the volume fraction η was assumed to be 0.95. On the other hand, the electromagnetic material parameters of the grains and the boundaries and the relative boundary thickness are identified. For identifying these parameters, an optimization problem is formulated and a non-linear least squares algorithm is used such that the fitted impedances match with the measurements [11]. The dielectric impedances of D1 and D2 and the magnetic impedances of T1 are used simultaneously with the inverse algorithm. All the material parameters are available in Table I, and they agree with the literature such that the inductive grains are conductive and the capacitive boundaries have a high resistivity [1], [2]. It was observed that the fitted impedances followed the same trend as the measurements mainly in the frequency range of 10 kHz - 10 MHz. In addition, there were discrepancies in the fitted dielectric and magnetic impedances below 10 kHz and above 1 MHz, respectively. It is emphasized that no measurements of the core T2 were used in the inverse algorithm for identifying the material parameters. Thus, T2 is used for validation. The simulated dielectric and magnetic impedances of T2 are compared against measurements in Fig. 3, and

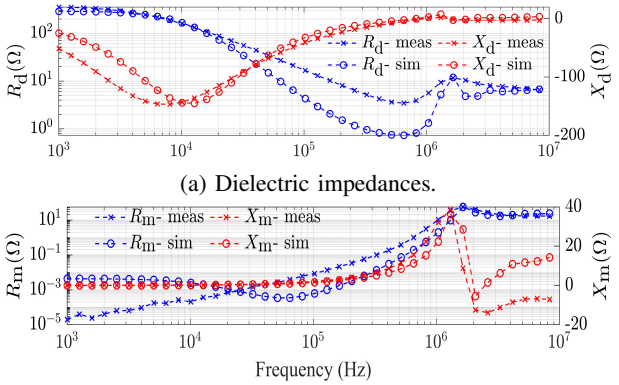

(a) Dielectric impedances.

(b) Magnetic impedances.

Fig. 3: Measured and simulated impedances of T2.

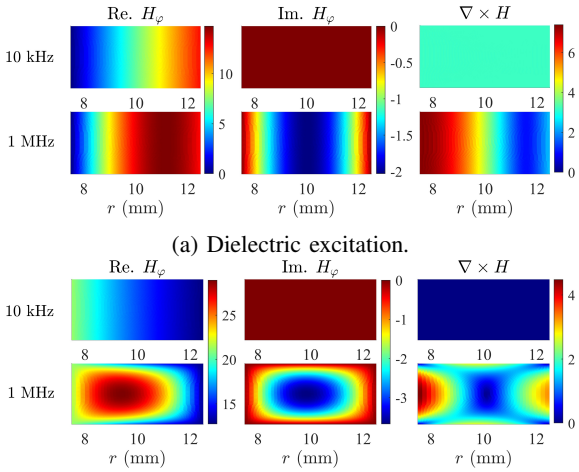

(a) Dielectric excitation.

(b) Magnetic excitation.

Fig. 4: The magnetic field H_φ (A/m) and the total current density $||\nabla \times \boldsymbol{H}||$ (kA/m^2) in the cross section of T2.

they follow the same trends as the measurements in the frequency range of 10 kHz - 1 MHz.

Field plots of the real and imaginary parts of the magnetic field H_φ (A/m) and the total current density $||\nabla \times \boldsymbol{H}||$ (A/m^2) in the cross section of the core T2 in dielectric and magnetic excitations at 10 kHz and 1 MHz are shown in Fig. 4. In both cases of dielectric and magnetic excitations, at 10 kHz, the imaginary part of the magnetic field is insignificant compared to the real part, which agrees with the typical distribution of the latter according to the inverse relation with the reluctance path. At 1 MHz, the imaginary part of the magnetic field becomes more significant and the real part has irregular distributions. Furthermore, the skin effect phenomenon can be observed from the current distribution at 1 MHz.

IV. Conclusion

The proposed approach is capable of modeling the dielectric and magnetic macroscopic behaviors of ferrite cores of different sizes and shapes. It was shown that the electromagnetic fields within the ferrite core behave similarly in dielectric and magnetic excitations, in the sense that the fields have typical distributions at low frequency but they become irregularly distributed at high frequency due to the dimensional effects. Furthermore, the proposed approach is very fast since it utilizes analytical formulas for the material models. Thus, it is considered as a practical approach for investigating ferrite cores while designing high-frequency magnetic components used in power electronic applications.

Acknowledgment

This project has received funding from the European Research Council (ERC) under the European Union's Horizon 2020 research and innovation programme (grant agreement No 848590). The Academy of Finland is also acknowledged for financial support (grants No 330062 and 346440).

References

[1] F. Fiorillo, C. Beatrice, O. Bottauscio and E. Carmi, "Eddy-Current Losses in Mn-Zn Ferrites," *IEEE Trans. Magn.*, vol. 50, no. 1, pp. 1-9, Jan. 2014.

[2] T. Dimier and J. Biela, "Eddy Current Loss Model for Ferrite Ring Cores Based on a Meta-Material Model of the Core Properties," *IEEE Trans. Magn.*, vol. 58, no. 2, pp. 1-5, Feb. 2022.

[3] M. Belkadi, B. Ramdane, D. Trichet and J. Fouladgar, "Non Linear Homogenization for Calculation of Electromagnetic Properties of Soft Magnetic Composite Materials," *IEEE Trans. Magn.*, vol. 45, no. 10, pp. 4317-4320, Oct. 2009.

[4] G. Meunier, V. Charmoille, C. Guerin, P. Labie and Y. Marechal, "Homogenization for Periodical Electromagnetic Structure: Which Formulation?," *IEEE Trans. Magn.*, vol. 46, no. 8, pp. 3409-3412, Aug. 2010.

[5] O. Bottauscio and A. Manzin, "Comparison of multiscale models for eddy current computation in granular magnetic materials," *J. Comp. Phys.*, vol. 253, pp. 1-17, Nov. 2013.

[6] I. Niyonzima, R. Sabariego, P. Dular and C. Geuzaine, "Nonlinear Computational Homogenization Method for the Evaluation of Eddy Currents in Soft Magnetic Composites," *IEEE Trans. Magn.*, vol. 50, no. 2, pp. 61-64, Feb. 2014.

[7] X. Ren, R. Corcolle, and L. Daniel, "Losses Approximation for Soft Magnetic Composites Based on a Homogenized Equivalent Conductivity," *AEM*, vol. 5, no. 2, pp. 59–64, Sep. 2016.

[8] J. Vesa, L. Hyvärinen and P. Rasilo, "Eddy-Current Loss Model for Soft Magnetic Composite Materials Considering Particle Size Distribution," *IEEE Trans. Magn.*, vol. 59, no. 7, pp. 1-8, July 2023.

[9] J. Vesa, "Complex Reluctivity and Dynamic Hysteresis Model for Soft Magnetic Composite Materials," arXiv:2408.11597.

[10] J. Lammeraner and J. Štafl, "Eddy Currents". London, U.K.: Iliffe Books Ltd., 1966.

[11] R. Elkhadrawy, J. Vesa, T. Tarhasaari, V. Tsakaloudi, and P. Rasilo, "2-D Axisymmetric FEM-Based Approach for Identifying Dimension- and Frequency-Independent Material Parameters of Mn-Zn Ferrites," *IEEE Trans. Magn.*, doi: 10.1109/TMAG.2024.3417357.